ARPA Order No. 22-62

TG 331-16
Copy No.
21

TASK R

Quarterly Progress Report No. 16
for the period
1 Jan. - 31 Mar. 1963

TASK R IS A PROGRAM OF RESEARCH IN PHYSICO-CHEMICAL AND FLUID DYNAMIC PHENOMENA BASIC TO THE UNDERSTANDING OF HIGH-TEMPERATURE, HIGH-SPEED GAS FLOW. IT IS SUPPORTED BY THE ADVANCED RESEARCH PROJECTS AGENCY THROUGH CONTRACT NOw 62-0604-c WITH THE BUREAU OF NAVAL WEAPONS, DEPARTMENT OF THE NAVY.

THE JOHNS HOPKINS UNIVERSITY
APPLIED PHYSICS LABORATORY
8621 GEORGIA AVENUE SILVER SPRING, MARYLAND

ARPA Order No. 22-62

TG 331-16

TASK R

Quarterly Progress Report No. 16
for the period
1 Jan. - 31 Mar. 1963

THE JOHNS HOPKINS UNIVERSITY
APPLIED PHYSICS LABORATORY
8621 GEORGIA AVENUE SILVER SPRING, MARYLAND

GENERAL OBJECTIVES OF TASK R

It seems likely that long-range development of improved propulsion systems will rely more and more upon a sound understanding and quantitative knowledge of the underlying physical and chemical phenomena involved. Many of these phenomena, and the practical problems arising in connection with them, have to do with the high temperatures characteristic of most advanced propulsion systems. Prediction of performance, the problems encountered with materials, heat transfer and cooling techniques - all these become more difficult and sophisticated with the trend to higher temperature operation, and will ultimately require a more fundamentally based understanding than is characteristic of the usual expensive "cut-and-try" or "quick-fix" test procedures.

Research performed under Task R at the Applied Physics Laboratory is intended to provide some of this basic knowledge in appropriate areas. The general emphasis is on the physico-chemical and fluid dynamic behavior of high temperature, high speed gas flows such as occur in most advanced propulsion systems.

A. A. Westenberg
Program Coordinator

SUMMARY

I. DISSOCIATED GAS STUDIES

(N. de Haas and A. A. Westenberg)

Objective

Several aspects of the high temperature gas flow associated with most propulsion systems have to do with the behavior of dissociated gases containing various labile atoms and radicals. Heat transfer and mixing processes often involve the diffusion of such species and their reactions in gas boundary layers and at surfaces. Because of their high reactivity, reliable basic data on the transport and kinetic propoerties of atoms and radicals are difficult to obtain. The difficulties lie both in establishing a well-defined experimental system appropriate to the measurement to be carried out and in detecting and measuring the labile species themselves.

The present program represents an effort, first of all, to utilize the flow tube technique to study the diffusion and chemical kinetics of discharge-generated atoms and radicals under well-defined conditions. The detection system to be employed is that of electron spin resonance (ESR), since the unpaired electron(s) possessed by all free radicals makes this technique the most widely applicable of any presently available. Thus the objective of this research is to acquire the necessary know-how in ESR as a quantitative detector of atoms and radicals, and to use it in appropriate diffusion and kinetic studies of such species.

Atom Concentration Measurements

In the previous progress report (Ref. 1) a preliminary comparison of NO_2 gas phase titration and the electron spin resonance (ESR) method of O-atom concentration measurement was presented. During the present quarter additional efforts were made to obtain better agreement between the two methods, but a check within 25% is the best result so far. Because of the difficulties involved in metering NO_2 (mostly due to the pressure dependent equilibrium between NO_2 and N_2O_4 and the small flows required) attention was turned to N-atom concentration measurements. In this case the ESR results (calibrated against known pressures of O_2) are to be compared with those of titration of N atoms with NO according to

$$NO + N \rightarrow N_2 + O$$

with the ESR spectrometer used to indicate the end-point, i.e. the disappearance of all N atoms.

Curve A of Figure I-1 shows the result of a typical titration. Peak values of the spectrometer signal were used to follow the relative concentrations of N. The flow system is that shown in Fig. I-1 of Ref. 1.

It is clear that the situation does not favor a satisfactory titration. A straight line as sketched for curve B should have been obtained. It appears that for small rates of NO injection into the $N + N_2$ mixture, the concentration of N-atoms in the cavity is greater than for no NO flow. For the data shown the distance from discharge to injection point was about 15 cm. If the discharge was moved further from the injection point the peak of curve A was lowered. However, the straight line B of a normal titration was still not obtained.

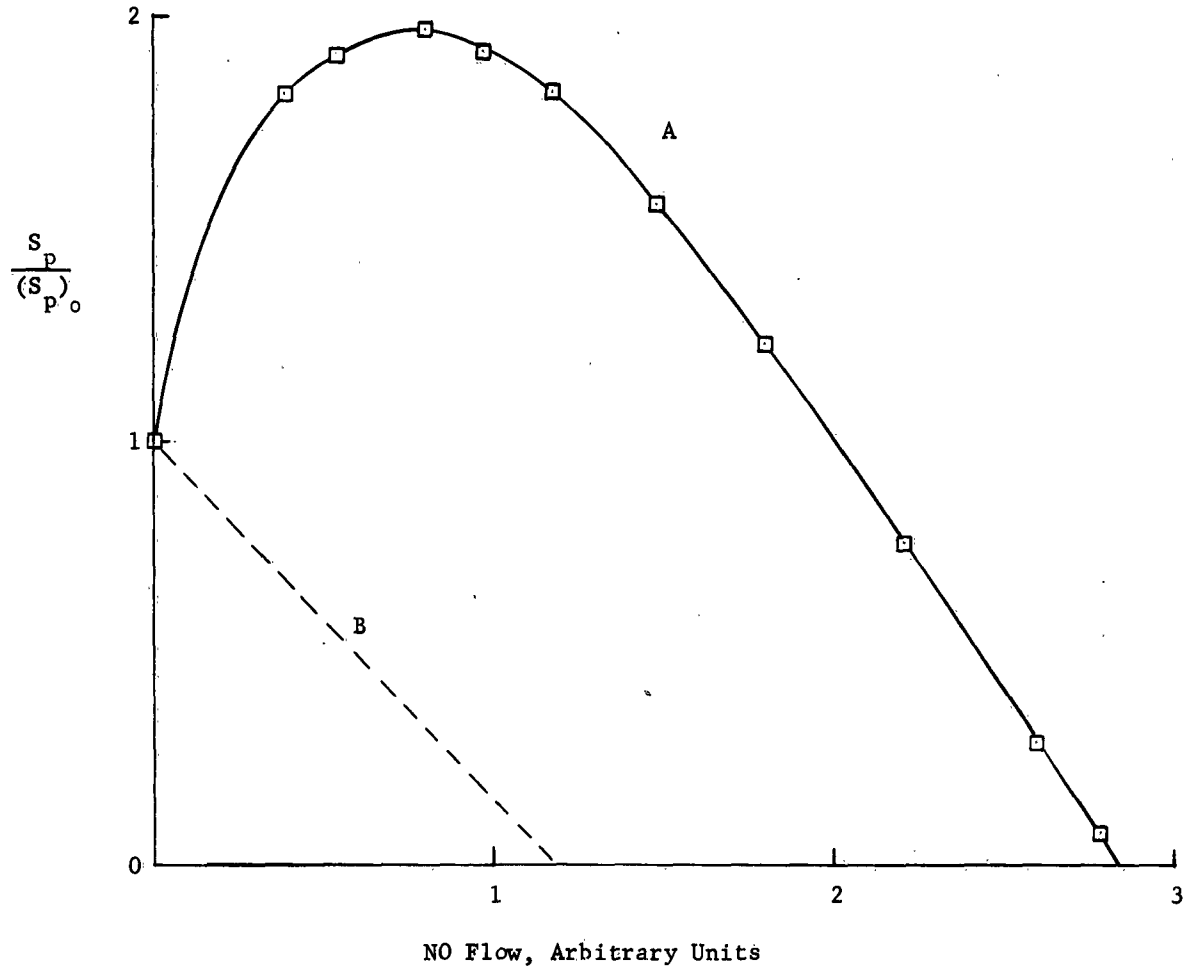

Fig. I-1. N-Atom Peak Signal Heights (S_p) as a Function of NO Flow into a Mixture of N + N_2. S_p is measured relative to the signal height for no NO flow. The NO flow at the peak of the curve is about 0.1% of the total flow. Dotted line B shows how ideal titration would behave.
Flow tube conditions: P = 7.9 mm Hg; $\dot{n}_{N_2} \simeq 1.66 \times 10^{-5}$ moles/sec; $\dot{n}_{NO} \simeq 2.4 \times 10^{-8}$ moles/sec (1 unit of NO flow)

There are various possible reasons for such behavior. (1) It is usually found that small amounts of "impurities" in a discharge-generated atom source increase the apparent output. Whether this is due to an actual increase in atom concentration from the discharge or a poisoning of the tube walls so that there is decreased atom loss on the way to the detector is not always clear. In the present case the ESR cavity and the titration point were located within a few centimeters of each other, and it is difficult to see how a wall effect could be very important under these flow conditions. It is also difficult to see how diffusion of NO back into the discharge could occur (calculation indicated the NO concentration should drop off by a factor of about e^{-38} for the existing conditions from NO inlet to discharge). Direct addition of NO to the N_2 flow upstream of the discharge did not cause appreciable change in the N-atom line peak height. On the other hand, the effect of increasing the distance between discharge and titration point seemed to reduce the increase in N-atom signal height upon NO addition, which might imply a back-diffusion into the discharge. (2) There is the possibility that some excited species coming out of the discharge dissociates the NO, giving more N-atoms than are normally detected without NO addition. This idea was discarded when the addition of O_2 instead of NO at the titration point also caused an increase in the N-atom signal. The increase was larger than with NO (about a factor of 4 over the no O_2 peak height). (3) It might be that both NO and O_2 (being paramagnetic) lead to higher rates of relaxation of N-atoms, assuming the possibility that the N-atoms were approaching a condition of microwave saturation in the first place. This question requires much more exploration, but it should be noted that the addition of Argon at the titration point also caused some increase in the N-atom line--although less pronounced than with NO and O_2. It is difficult to see how Argon could provide for more efficient relaxation in this case.

This whole question is very much unresolved at present and is being investigated further.

Theory of Spectrometer Signals

Wahlquist (Ref. 2) has recently derived relationships among certain characteristics of spectrometer signals of single unsaturated Lorentzian absorption lines with arbitrary modulation. The results that will be of use in this study are presented here in summary form. The notation used is primarily that of Ref. 3.

An unsaturated Lorentzian absorption line has a shape given by

$$G(H - H_0) = \frac{1}{\pi} \frac{\frac{1}{2}H_{\frac{1}{2}}}{(\frac{1}{2}H_{\frac{1}{2}})^2 + (H - H_0)^2} \qquad (1)$$

which satisfies the normalization condition

$$\int_0^\infty G(H - H_0)\, d(H - H_0) = \frac{1}{2} \qquad (2)$$

In these equations $H_{\frac{1}{2}}$ is the full-width at half-height of the line and H_0 is the resonant field intensity. See Fig. I-2.

The intensity of a line I_0 is given by the area under the true absorption curve. I_0 is a quantity which is inversely proportional to the temperature and proportional to the transition probability, the absorbing component concentration, and various instrumental parameters. The spectrometer actually gives a signal S(H) which is the phase detected absorption line as distorted by

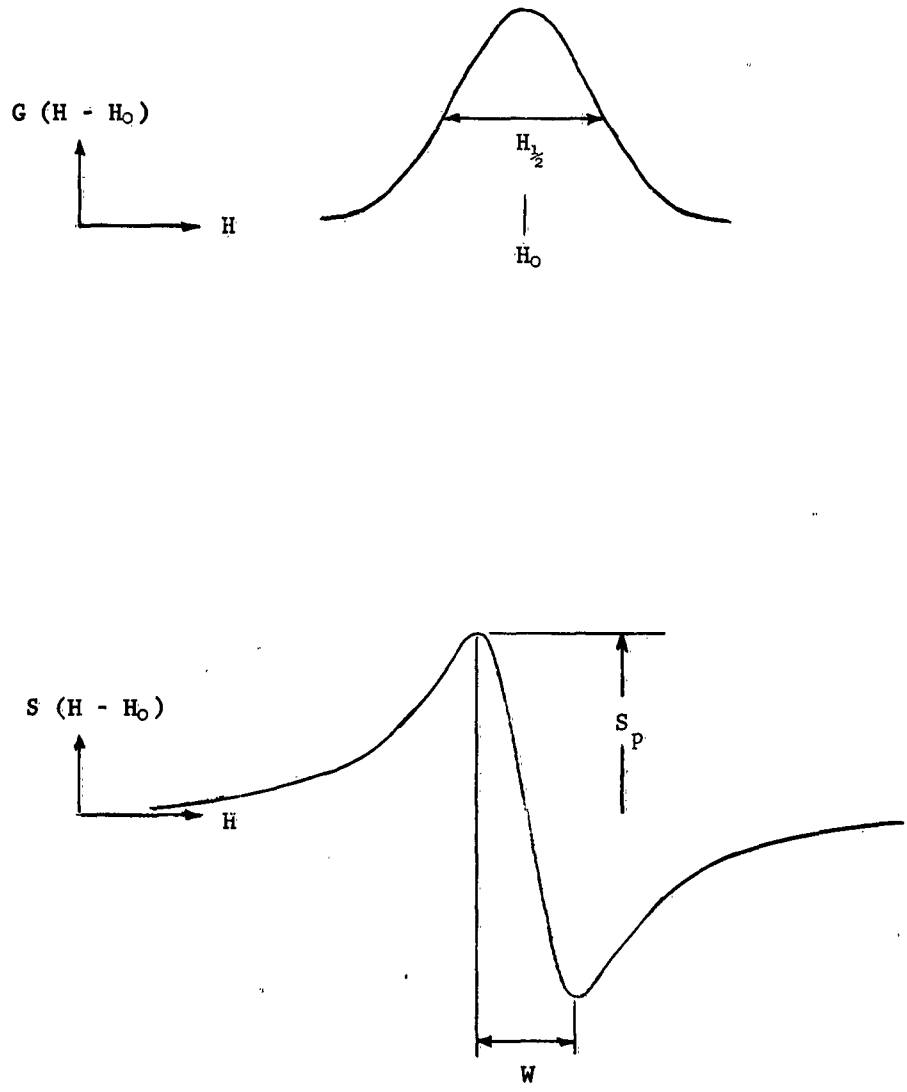

Fig. I-2. Sketch of an ESR Absorption Line and Its Corresponding Spectrometer Signal.

finite amplitude modulation M. Wahlquist has shown that for any M, the double integral I is related to the true intensity by

$$I = \int_{-\infty}^{\infty} dH \int_{-\infty}^{H} S(H)\, dH = MI_0 \qquad (3)$$

In terms of quantities of primary interest at a given temperature, we may write

$$I = C\, M\, N\, F \qquad (4)$$

where N is the concentration (moles/cm^3) of the absorbing species, F is the transition probability involved, and C is a constant.

Halbach (Ref. 4) has shown that, for any M, the double integral may be obtained from a single integration by means of

$$I = \int_{-\infty}^{\infty} H\, S(H)\, dH \qquad (5)$$

Although measurements of the concentration of atoms may be made through use of Eqs. 4 and 5, it would be far more convenient to use the spectrometer signal directly rather than its double integral. The peak spectrometer signal, S_p, and the width between peaks, W, (see Fig. I-2) have been shown in Ref. 3 to be useful in this regard.

For any modulation amplitude, M, the peak spectrometer signal for a single line is

$$S_p = \pm D \frac{N}{H_{\frac{1}{2}}} F \left[\frac{U_p - 2}{U_p (2U_p - 3)} \right]^{\frac{1}{2}} \tag{6}$$

where $U_p = 2 + \frac{4}{3}\beta^2 + \frac{4}{3}\beta^2(\beta^2 + \frac{3}{4})^{\frac{1}{2}}$ and $\beta = H_{\frac{1}{2}}/2M$. D is a constant for a given set of spectrometer conditions.

The width between signal peaks, W, is given by

$$\frac{W}{H_{\frac{1}{2}}} = \frac{1}{\beta} \left[1 + \frac{5}{3}\beta^2 - \frac{4}{3}\beta (\beta^2 + \frac{3}{4})^{\frac{1}{2}} \right]^{\frac{1}{2}} \tag{7}$$

In the case of low modulation, i.e. small $M/H_{\frac{1}{2}}$, Eq. 6 becomes

$$S_{p\ell} = \pm D \frac{NF}{(H_{\frac{1}{2}})^2} M \tag{8}$$

and Eq. 7 reduces to

$$W_\ell = \frac{H_{\frac{1}{2}}}{\sqrt{3}} \tag{9}$$

If the modulation amplitude is set such that the maximum Sp is obtained, then

$$M_m = H_{\frac{1}{2}} \tag{10}$$

$$S_{pm} = \pm D \frac{NF}{H_{\frac{1}{2}}} \tag{11}$$

and

$$W_m = \sqrt{3}\ H_{\frac{1}{2}} \tag{12}$$

It is also noted that at very large $M/H_{\frac{1}{2}}$

$$W_L = 2\ M \tag{13}$$

so that the signal width is independent of pressure (i.e. $H_{\frac{1}{2}}$).

Following are other relationships which will be of use. They are obtained from the foregoing equations.

When applied to single lines of two absorbing species, a and b, using the same low M for both, Eqs. (8) and (9) give

$$\frac{N_a}{N_b}\frac{F_a}{F_b} = \frac{(S_\ell)_a}{(S_\ell)_b}\ \frac{(W_\ell)_a^2}{(W_\ell)_b^2} \tag{14}$$

Similarly, Eqs. (11) and (9) give

$$\frac{N_a}{N_b}\frac{F_a}{F_b} = \frac{(S_m)_a}{(S_m)_b}\ \frac{(W_\ell)_a}{(W_\ell)_b}\ ; \tag{15}$$

The basic line width $H_{\frac{1}{2}}$ is presumed to be proportional to the total pressure in the system in the millimeter (pressure broadening) regime. This is reasonable if the absorbing species is present at low concentration.

Experimental Tests of the Theory

The theory of the previous section was developed for absorption lines having Lorentzian shapes. Table I-1 shows the measured shapes of the J=1 O-atom line and an O_2 line (K=5, J=4→6, M=1→2) taken at low modulation in comparison with Eq. (1).

Table I-1. Shape of the O (J=1) Line and the O_2 (K=5, J=4→6, M=1→2) Line. System: $O + O_2$, P = 0.35 mm Hg.

	$\frac{H - H_0}{W}$ (Lorentzian)	$\frac{H - H_0}{W}$ (Experimental)	
S/Sp		O (J=1)	O_2 (K=5, J=4→6, M=1→2)
1.0	1.00	1.00	1.00
0.8	1.65	1.63	1.68
0.6	2.10	2.12	2.11
0.4	2.75	2.88	2.68
0.2	3.80	3.88	3.55
0.1	5.00	5.10	4.80

It is seen that the two lines are nearly Lorentzian.

The assumption that $W_\ell \propto H_{\frac{1}{2}} \propto$ pressure was tested on an O_2 line. The results are given in Table I-2. The check is satisfactory.

Table I-2. Dependence of $W_\ell \propto H_{\frac{1}{2}}$ on the Total Pressure, P.

(System: O_2)

P (mm Hg)	P/P_o	$W_\ell/(W_\ell)_o$
.54	1.00	1.00
1.00	1.85	1.76
1.49	2.76	2.55
1.94	1.00	1.00
4.23	2.18	2.13
1.23	1.00	1.00
2.02	1.64	1.69

The general equations for the peak signal, Eq. (6), and peak-to-peak width, Eq. (7), are plotted in Figs. I-3 and I-4, respectively. Also shown in these figures are the experimental data obtained on the O_2 (K=5, J=4→6, M=1→2) line at a pressure of 2.46 mm Hg. Because of a lack of knowledge of the absolute modulation amplitude M the data were fitted to the theoretical curves at $1/\beta = 1.40$. The fit to the S_p curve is excellent to somewhat beyond maximum S_p ($1/\beta = 2.00$), but the fit to the W curve is somewhat less satisfactory, perhaps because the widths are harder to measure.

Eq. (6) provides for a comparison with respect to transition probabilities of pure lines at the same M which have equal $H_{\frac{1}{2}}$ values. For constant pressure of the species giving rise to the lines, the use of the same M for all lines will make β the same.

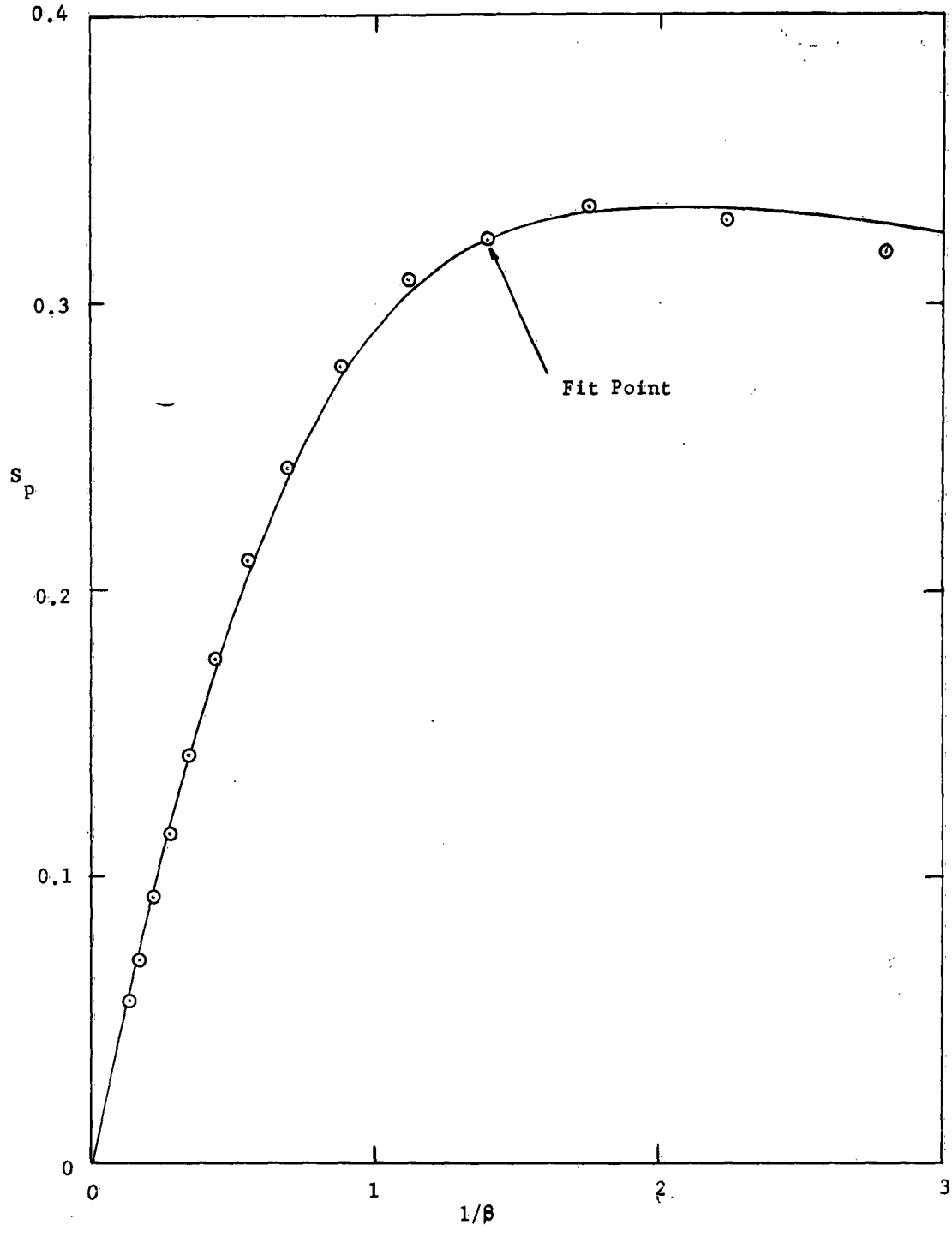

Fig. I-3. Peak Spectrometer Signal (S_p) as a Function of the Ratio of Modulation to Signal Width. $1/\beta = 2M/H_{\frac{1}{2}}$. Line - theoretical (Eq. 6). Points - experimental for system O_2, P = 2.46 mm Hg.

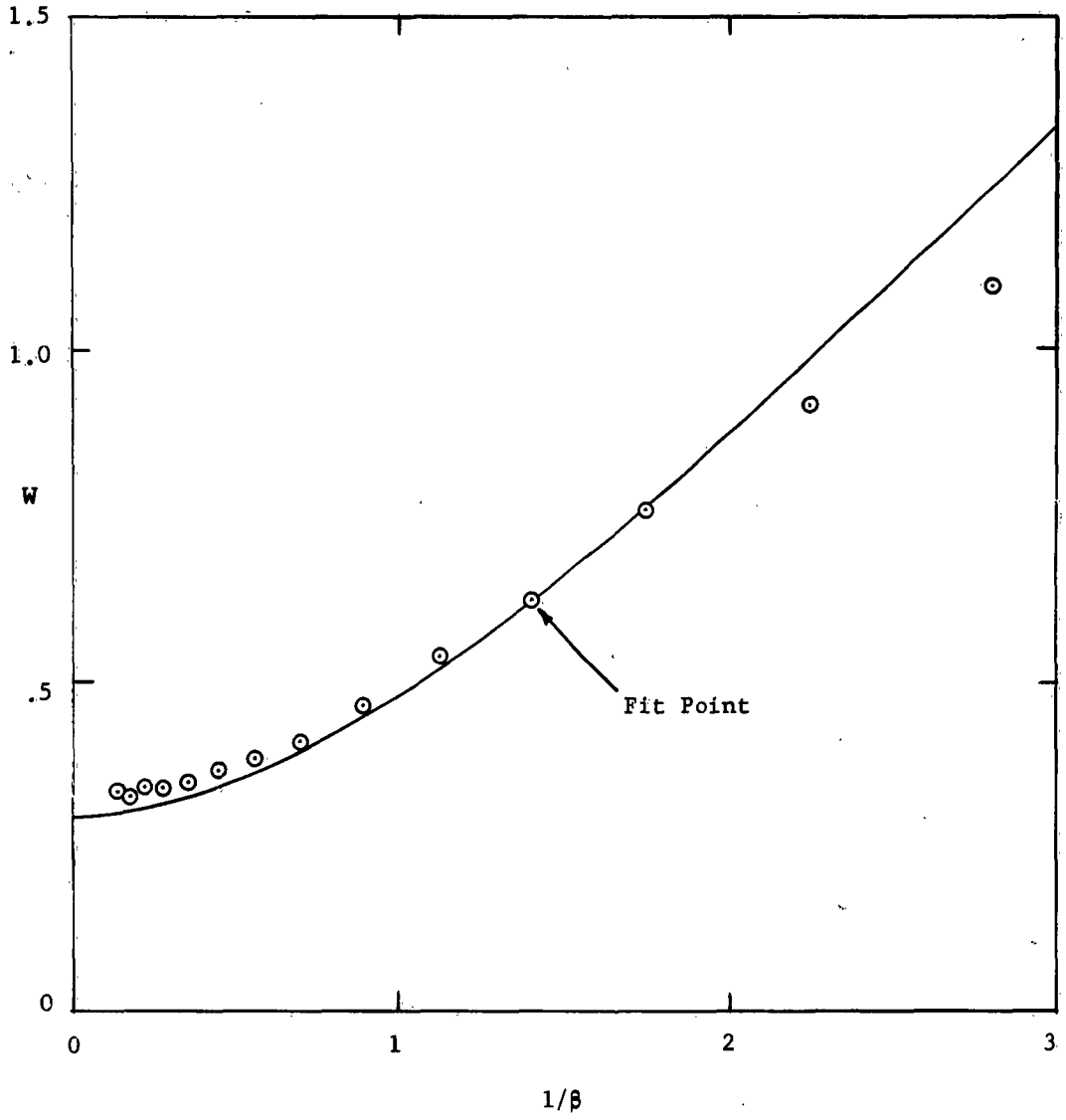

Fig. I-4. Spectrometer Signal Width (W) as a Function of the Ratio of Modulation to Signal Width. $1/\beta = 2M/H_{\frac{1}{2}}$. Line - theoretical (Eq. 7). Points - experimental for system O_2, P = 2.46 mm Hg.

In Eq. (6), U_p is thus a constant and S_p is proportional only to the transition probability. This is demonstrated in Table I-3 where various O_2 lines are compared as to S_p. The theoretical transition probabilities were obtained from Ref. 5. Agreement of the measured signal ratios with theory is excellent.

Table I-3. Comparison of S_p with Theoretical Transition Probabilities of Various O_2 Lines. (System: O_2, P = 0.39 mm Hg)

Line Pair	Experimental Peak Ratio	Theoretical Ratio
a/b	0.094	0.092
a/c	0.047	0.046
a/d	0.028	0.028
a/e	0.024	0.023
b/c	0.497	0.500
b/d	0.298	0.306
b/e	0.251	0.247
c/d	0.602	0.612
c/e	0.505	0.495
d/e	0.840	0.808

O_2 Line Identification:

a K=3, J=2→4, M=1→0
b K=5, J=4→6, M=1→2
c K=1, J=1, M=-1→2
d K=1, J=2, M=1→2
e K=1, J=2, M=0→1

For relative measurements of atom concentrations at constant total pressure, Eq. (6) predicts that S_p at a fixed M should be proportional to N. Similarly, Eq. (4) requires the integrated quantity I, obtained from Eq. (5), to be proportional to N. By varying the distance between discharge and cavity, the O-atom concentration was varied at constant pressure (0.58 mm - low enough for resolution of the J=1 and J=2 lines). Signal heights and integrals for both J=1 and J=2 lines were obtained at a fixed M=63, and signal heights alone at another M=200 (arbitrary units). The relative values are compared in Table I-4. The signal height ratios generally agree well between J=1 and J=2 at the same and different modulations. The integrals are in fair agreement, but are much harder to evaluate numerically - which probably accounts for the discrepancies. There may also have been some variation with time of the atom concentration during the required data taking period.

Table I-4. Comparison of Relative O-Atom Concentrations Measurements by Peak Heights and Integrals. System: O + O_2 at 0.58 mm Hg.

M = 63				M = 200	
I/I_o (J=1)	I/I_o (J=2)	$S_p/(S_p)_o$ (J=1)	$S_p/(S_p)_o$ (J=2)	$S_p/(S_p)_o$ (J=1)	$S_p/(S_p)_o$ (J=2)
1	1	1	1	1	1
.90	---	.83	.83	.86	.86
.72	.79	.77	.78	.79	.78
.16	.19	.17	.17	.18	.18

Various tests of the limiting cases represented by Eqs. (8)-(12) have been carried out. These tests are listed below.

(a) Eq. (8) states that $S_{p\ell}/M$ and W_ℓ should be a constant at low modulations and constant pressure. This is shown to be the case in Table I-5 for the K=5, J=4→6, M=1→2 line of O_2.

Table I-5. Dependence of $S_{p\ell}$ and W_ℓ on Modulation (System: O_2, P = 2.94 mm Hg)

M	$S_{p\ell}/M$	W_ℓ
50	1.80	7.0
64	1.80	7.0
82.5	1.78	7.0
98	1.74	7.0
125	1.78	7.0
160	1.76	7.2
200	1.72	7.5

Similar data were also obtained for the J=1 line of O atom and for the composite J=2 line of O atom.

(b) Eq. (11) states that the maximized signal S_{pm} for a pure gas like O_2 is independent of pressure, since both N and $H_{\frac{1}{2}}$ are proportional to pressure. This was shown to be true for two pairs of pressures using the line K=5, J=4→6, M=1→2. Table I-6 gives these results.

Table I-6. Dependence of S_{pm} on Pressure. (System: O_2)

P (mm Hg)	S_{pm} (arbitrary units)
1.23	1.10
2.02	1.13
0.45	0.55
4.97	0.54
1.94	0.48
4.23	0.47

Limited checks on Eqs. (14) and (15) have also been made.

Relative and Absolute Concentration Measurements

It was shown in the previous two sections that an adequate theory exists to relate spectrometer signal peaks to relative concentrations. The inaccurate and inconvenient computation of double integrals of the signal is thereby avoided. In general, only relative concentrations will be needed for the intended gas diffusion measurements. In many of the anticipated experiments involving O-atoms it will be convenient to use the composite J=2 line because of its much larger signal compared to a J=1 line. The theory outlined here is not directly applicable to a composite line, but Barth, et al (Ref. 3) have shown that under certain conditions the general form of the single line equations also hold for the composite line.

Absolute atom concentration measurements remain to be tested by independent means, though the theory is developed.

References

1) Task R Quarterly Report No. 15, The Johns Hopkins University, Applied Physics Laboratory Report No. TG-331-15.

2) H. Wahlquist, J. Chem. Phys. 35, 1708 (1961).

3) C. A. Barth, A. F. Hildebrandt, and M. Patapoff, Dis. Faraday Soc. No. 33, 162 (1962).

4) K. Halbach, Phys. Rev. 119, 1230 (1960).

5) M. Tinkham and M. W. P. Strandberg, Phys. Rev. 97, 951 (1955).

II. ROCKET NOZZLE FLUID DYNAMICS

(F. K. Hill and H. J. Unger)

Objective

Experimental data have been collected on which to base an understanding of the fluid dynamic processes which take place in rocket nozzles. Solid propellants generate a high-temperature gas that forms a complex fluid system during its passage from the combustion chamber to the nozzle and rapidly expands into supersonic flow. Due to the fact that the gas is composed of a mixture of substances, the fluid properties are difficult to predict precisely. For this reason, it has been considered worth while to acquire experimental data on chemical reaction rates, the concentration of species, boundary layer characteristics, suface reaction and heat transfer rates of the gas.

Techniques developed for use in supersonic and hypersonic wind tunnels have been used to gather experimental boundary layer data in the supersonic section of the rocket nozzle. Detailed boundary layer properties may be used to accurately compute skin friction and heat transfer coefficients as functions of non-dimensional parameters such as Reynolds number, Mach number, etc. These coefficients provide the fundamental data for the design and fabrication of improved nozzles. The environmental conditions at the throat of the nozzle are so severe that one cannot employ conventional fluid dynamic measuring equipment. For this reason, one searches for other techniques for the determination of heat transfer properties.

Present experiments with the rocket tunnel have been conducted with a double-base propellant, ARP, manufactured by the Allegany Ballistics Laboratory. During combustion at 1100 psig and 2500°K, carbon dioxide, carbon monoxide, water vapor, hydrogen, and nitrogen are generated as the principal components of the gas. The first three of these components are active infrared absorbers in the spectral region, 4 to 6.5μ. In order to determine the composition of the gas mixture as it passes through the nozzle, an infrared absorption technique has been adapted for observing the flow at various stations. This system avoids any interference with the flow and is limited only by the gas sensitivity to the radiation that is transmitted through the flow. Absorption measurements of the gases are undertaken for the purpose of determining their concentration as well as their temperature. The infrared technique has been developed to utilize not only absorption, but emission properties as well. This method of observation is expected to be used on propellants with combustion temperatures in the area of 3500° to 4000°K. The species evolved in the combustion of these higher energy propellants are more numerous, more complicated, and include appreciable fractions of solid particles and free radicals.

A series of thirteen tests were run during this period at which time emission and absorption spectra were recorded separately at five stations in the nozzle. The results from these tests provide a striking comparison of the change in spectral response of the gas mixture over a range of temperatures from 1800°K down to 900°K.

Spectrographic Results

Reference 1 reviewed the testing procedure and some of the problems associated with recording the absorption spectra at various stations in the nozzle. In particular, the flushing problem was

discussed and spectra of both absorption and emission were shown. In order to separate absorption and emission effects the spectrometer was modified to accommodate a second chopper. This segmented wheel was placed close to the light source, so that the light from the source was chopped and provided an A.C. signal which could be absorbed by the tunnel gas. Any emission from the gas would then appear as a D.C. signal and not be recorded by the spectrometer. For emission measurements the source was turned off and the emission from the gas was converted to an A.C. signal by the chopper in front of the entrant slit of the spectrometer. The placement of these choppers is shown schematically in Fig. II-1.

In previous tests the problems relating to the correct flushing pressure with which to supply the slit windows in the nozzle test section were studied (Ref. 1). It was known that too low a flushing pressure - one which just matched or slightly exceeded the stream static pressure - allowed test section gases to enter and cool in the window ports. This was evident from the composite nature of the CO_2 spectra at 4.3μ where cold gas and hot gas spectra were superimposed. On the other hand, it was though that too high a flushing pressure caused the flow to separate in the nozzle, deflecting the stream and giving a distorted cross section for the light path. However, after analysis of previous results, it appeared that if this effect occurred, it was of secondary importance, and that the entrance of gas into the window ports was much more serious in its effects. Consequently, after Test No. 171, the first in this series, the N_2 flushing pressure to the window ports was increased to give higher flush pressures at the beginning of runs than used previously. This N_2 flush supply was programmed to decrease during the run to give window port pressures just slightly above the static stream pressure at the end of the run. Thus, it was hoped that any degradation of the spectra by gas entering the window ports could be recognized from comparison of successive frames of the photographic records.

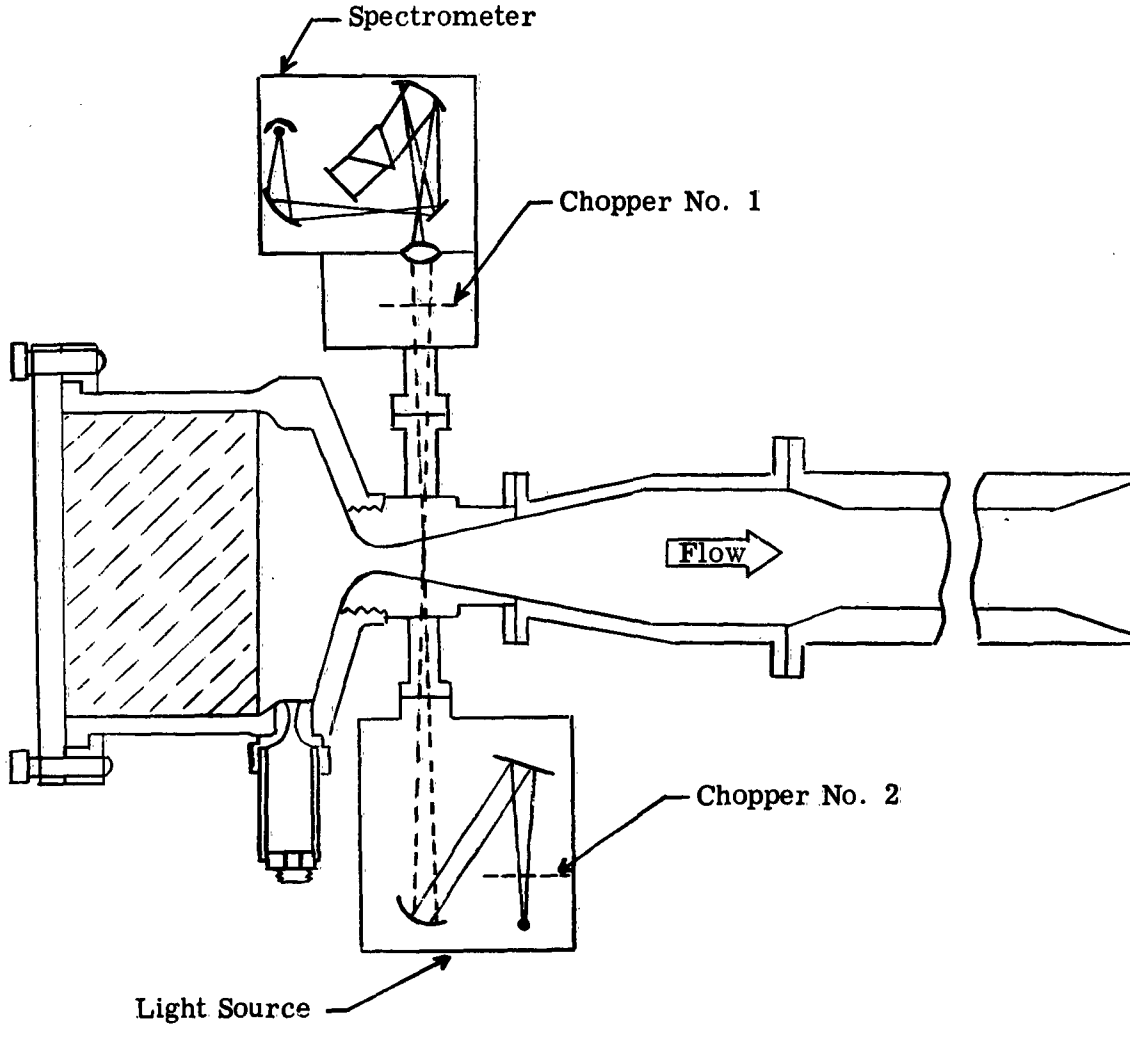

Fig. II-1 CHOPPER ARRANGEMENT FOR SPECTROMETER - NO. 1 FOR EMISSION (SOURCE OFF), NO. 2 FOR ABSORPTION (NO. 1 OPEN AND STOPPED)

The results of the tests are presented in Fig. II-2 (as recorded). This figure shows contact size prints made from one frame of the 35 mm films which photographed the oscilloscope displays. An absorption and an emission result is given for each station of measurement as indicated in the legends. It can be seen that the CO_2 absorption is large and saturates at 4.25μ for all stations except the first two. The emission, on the other hand, increases very markedly with temperature, and it should be noted that the amplitude of the signal was reduced for two of the emission tests to keep the spectrum on the screen. The locations of the stations in the nozzle are shown in Fig. II-3.

Emission Spectra. Figure II-4 depicts the measured amplitude of CO_2 at 4.25μ and 4.45μ, of CO at 4.82μ and of H_2O at 5.52μ and 5.93μ. The temperature, used as abcissa in Fig. II-4 and as listed in Fig. II-2, was calculated by numerical integration of the flow properties of the gas throughout the nozzle. It is the equilibrium value, and the method has been described in detail in Ref. 2. In Fig. II-4 the insert in the upper left-hand section illustrates the area observed in each test. Since the optical system is focused at the center of the test section, the same amount of gas (or same number of radiating molecules) are scanned at each station. Thus, the emission is dependent only on the temperature, gas composition, self absorption, and emissivity. It is planned to extend the emissivity calibration work so that the composition may be found from data as given in Fig. II-4.

Absorption Spectra. Figure II-5 presents the absorption measurements of CO_2 at 4.26μ, CO at 4.82μ and H_2O at 5.49μ, while Fig. II-6 gives CO_2 at 4.34μ, and H_2O at 5.65μ. Since the percentage composition of CO is comparatively large, the CO results are plotted separately on Fig. II-7. The independent variable used in these plots

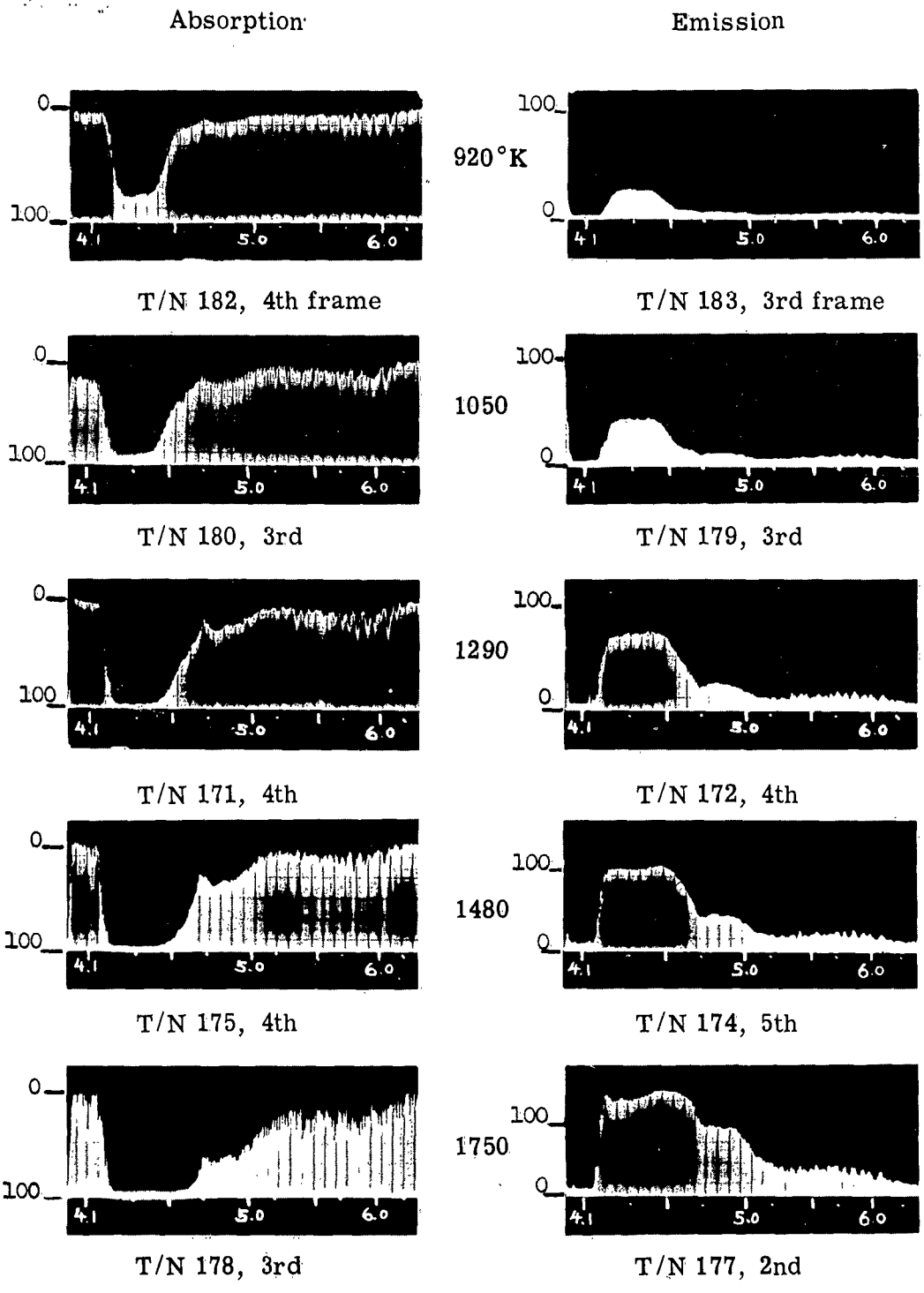

Fig. II-2. ABSORPTION AND EMISSION SPECTRA (4μ to 6.5μ) AT FIVE STATIONS IN ROCKET NOZZLE

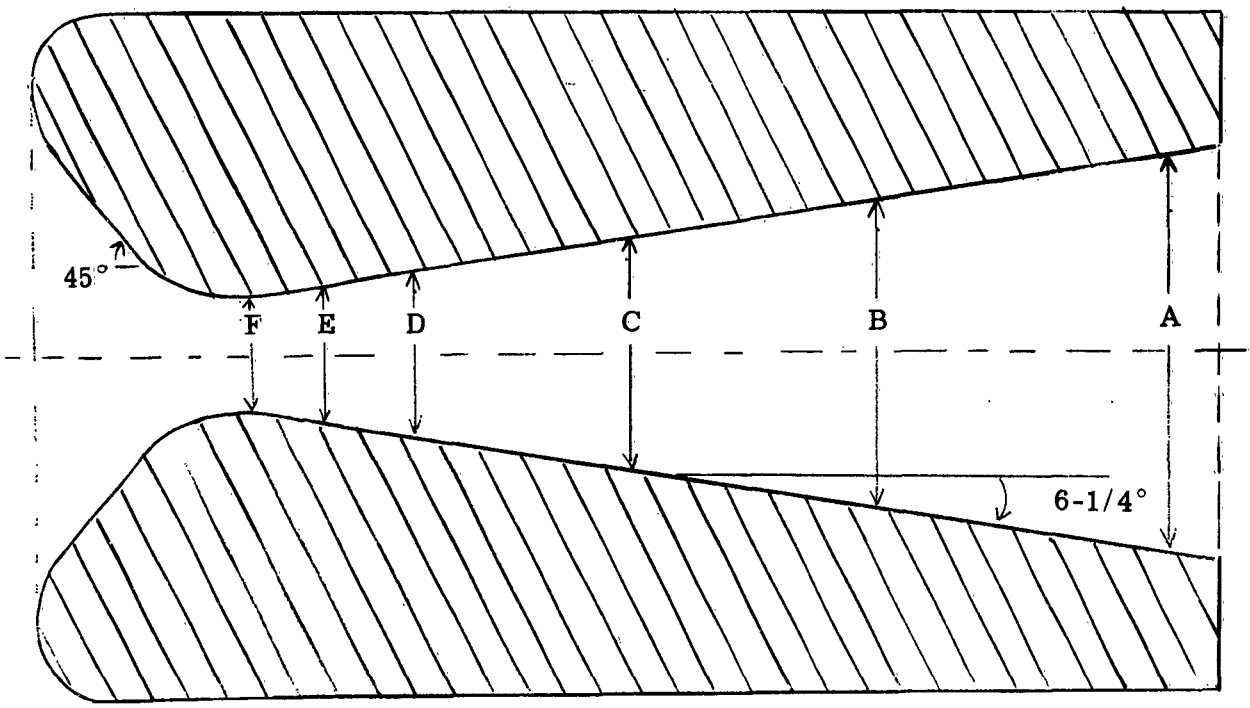

Station	Diameter (Inches)
A	2.33
B	1.86
C	1.348
D	1.06
E	0.803
F	0.630

Fig. II-3 NOZZLE DIMENSIONS AT THE FIVE TEST STATIONS WHERE ABSORPTION AND EMISSION SPECTRA WERE TAKEN

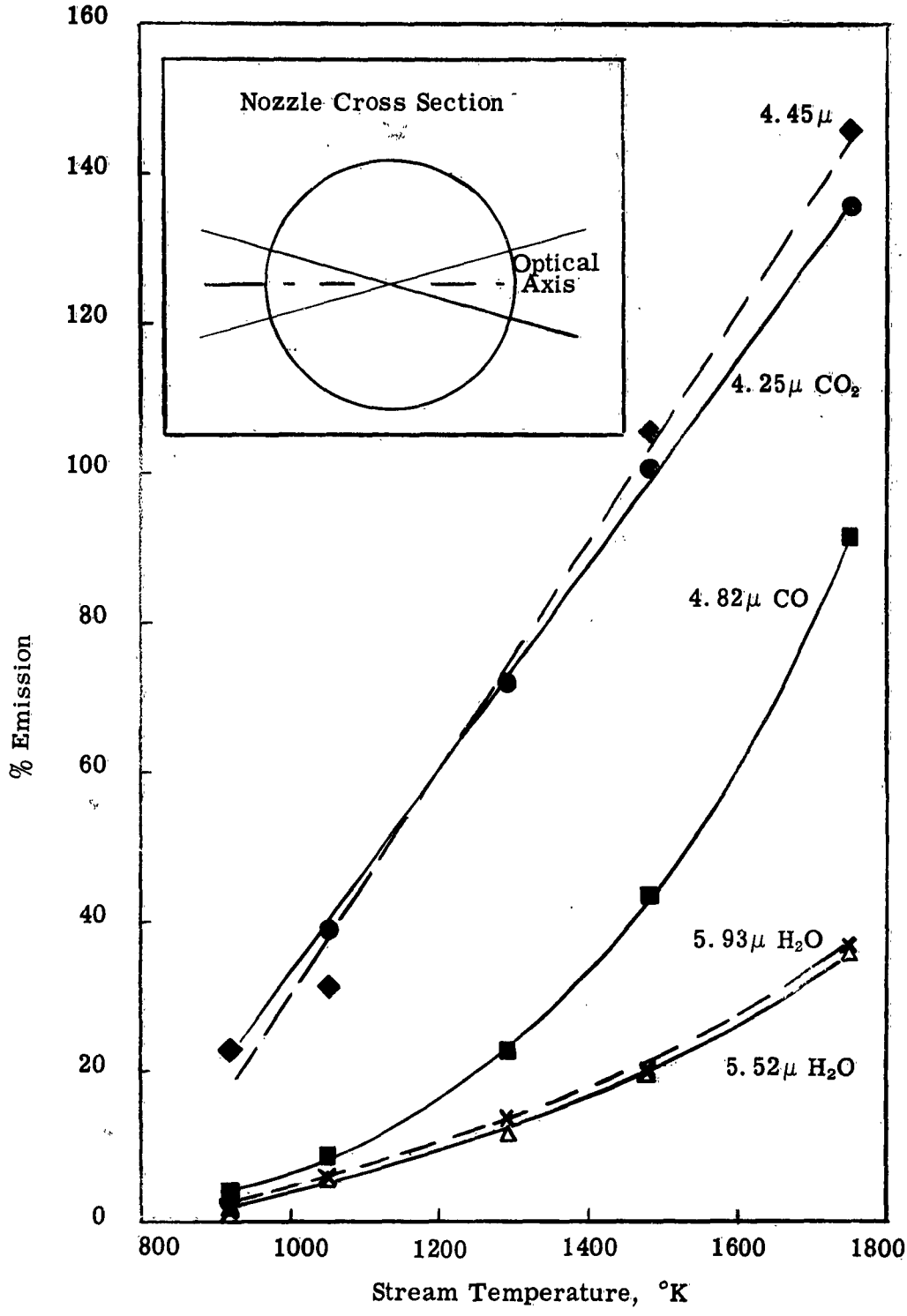

Fig. II-4 MEASURED EMISSION AMPLITUDE AS A FUNCTION OF TEST SECTION TEMPERATURE

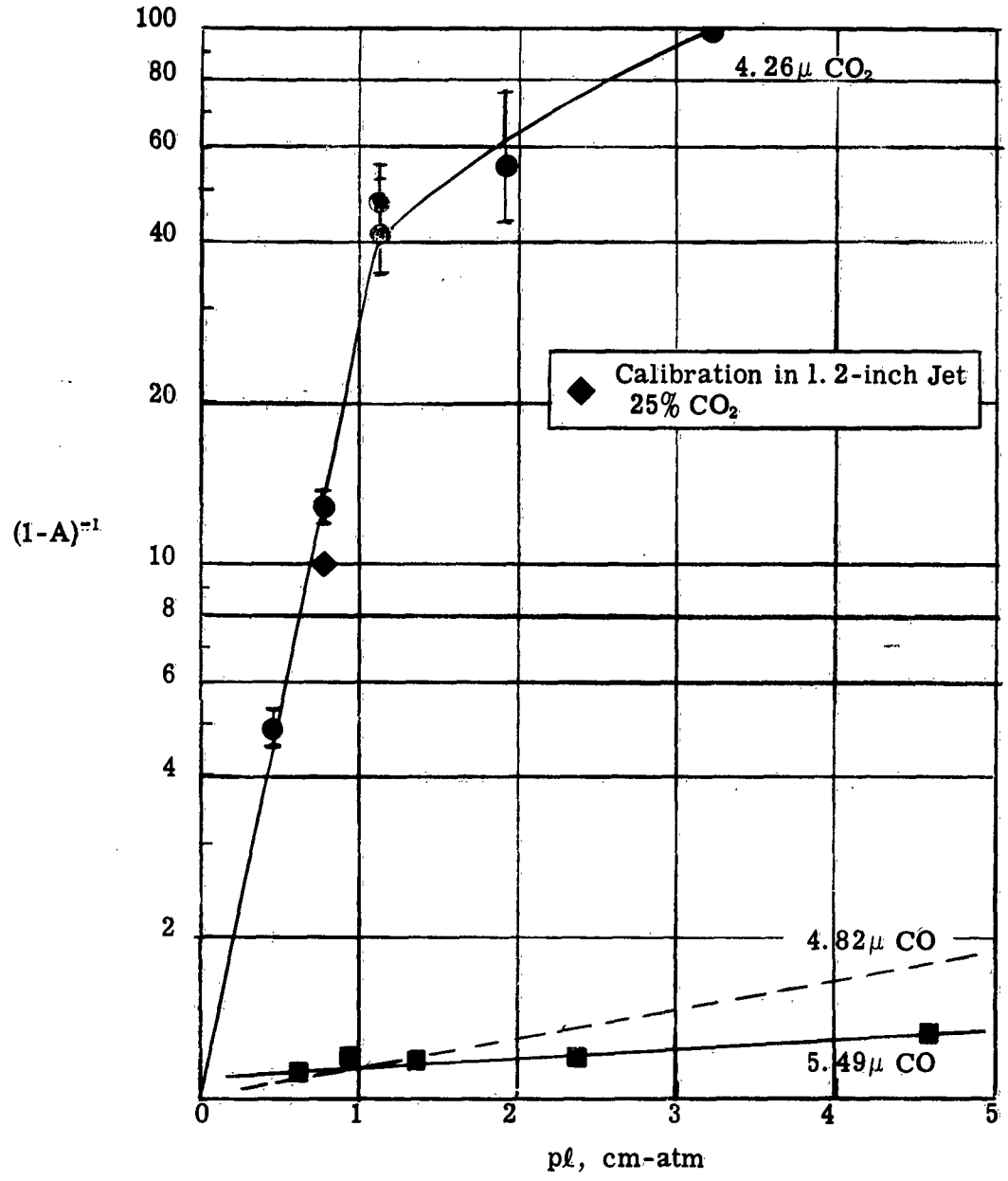

Fig. II-5 4.26μ ABSORPTION OF CO_2 IN ROCKET NOZZLE TEST SECTION FROM 920°K TO 1750°K

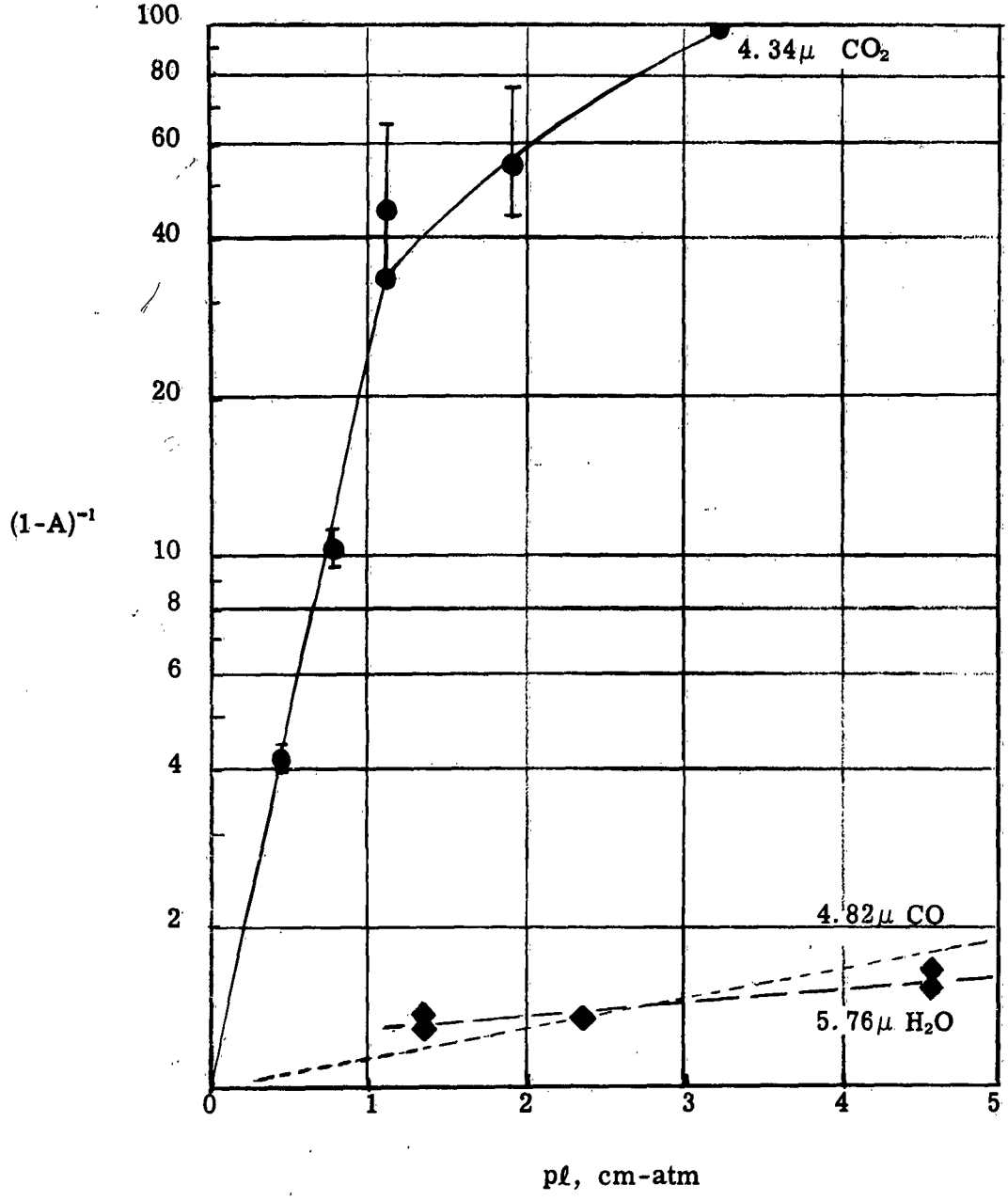

Fig. II-6 ABSORPTION OF 4.34μ CO_2 BAND IN ROCKET NOZZLE FROM 920°K TO 1750°K

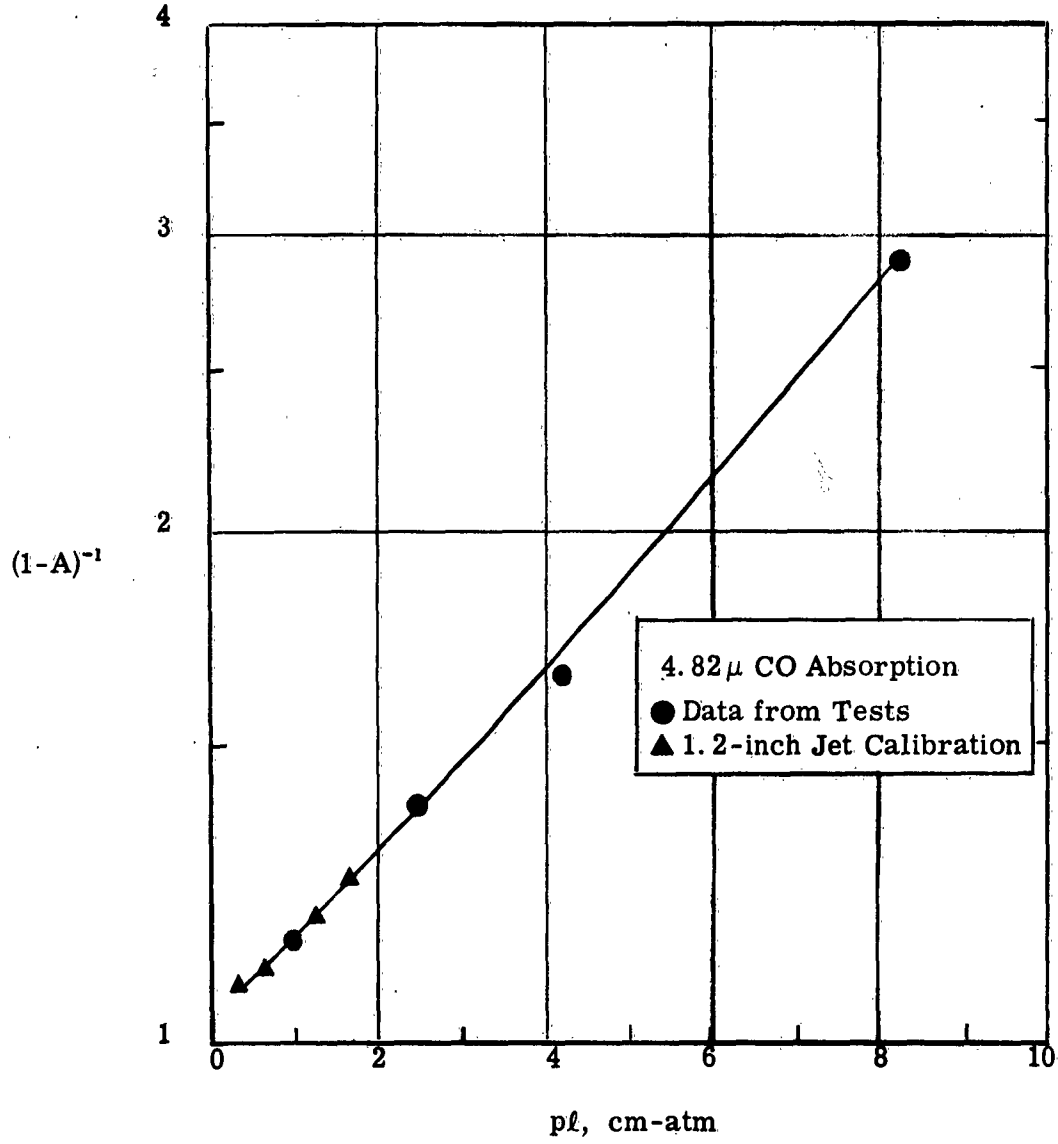

Fig. II-7 CO ABSORPTION IN 12.5° ROCKET NOZZLE

is $p\ell$ in cm-atm, where p is the pressure and ℓ is the optical path. Figure II-5 and II-7 also show calibration data made in a 1.2-inch rectangular jet using preheated mixtures of CO_2 and N_2, and CO and N_2. The ordinate of these graphs is $(1-A)^{-1}$ plotted logarithmically where A is the measured absorption. The linear behavior indicates the region where the Beer-Lambert law is valid. A computation of the absorption coefficient, k, for CO_2 at 4.26μ and 4.34μ for the data points given in Figs. II-5 and II-6 is shown in Table I.

Table I. CO_2 Absorption Coefficient

			4.26μ		4.34μ	
T/N	Temp.	$p\ell$	A	k	A	k
180	1050°K	0.775 cm-atm	92.2%	3.29	90.3%	3.01
182	920	0.512	79.5	3.46	76.0	3.13

These values may be compared to other data as follows:

1. k = 2.90 to 3 at 1200°K, λ = 4.40μ, Steinberg and Davies (Ref. 3)
2. k = s/d = 2.50 at 1200°K, λ = 4.40μ, Plass (Ref. 4)
3. k = 2.5 at 1200°K, λ = 4.25μ, Ferriso (Ref. 5)
   k = 3.3 at 1200°K, λ = 4.35 μ

From these tests it is concluded that absorption measurements for CO_2 at stations where the stream temperature is less than 1200°K will give a valid measure of the composition using the straight line portion of Figs. II-5 and II-6. The Beer-Lambert law with an

absorption coefficient of 3 appears to be a useful approximation and as accurate as the measurements justify. For all temperatures above 900°K the emission spectra provide a measure of the gas composition; but before quantitative values of composition can be derived, either the emissivity of the gas must be determined as a function of wavelength and temperature, or an applicable set of calibration data must be obtained by using simple mixtures at different composition, optical paths and temperatures.

The CO measurements of both absorption and emission provide useful data for composition determination at temperatures above 1000°K. The linear character of the absorption as given in Fig. II-7 looks most promising, and, again, the calibration of the test gas in the 1.2-inch jet corroborated the values obtained and the linear character of the absorption. It would be desirable to have a much larger calibrating jet to increase the optical path for the CO. However, handling copious quantities of this gas is a problem, even in the well ventilated test cell.

The H_2O measurements are somewhat uncertain because of the noise present during the absorption tests. However, the emission data appear consistent, and efforts will be made to provide calibration data by which they can be translated to composition determinations. The data for H_2O absorption indicate that emission measurements should be restricted to temperatures above 1000°K, whereas the absorption is appreciable to at least 100°K lower temperatures.

References

1. Task R Quarterly Progress Report No. 15, APL/JHU Report No. TG 331-15, for the period 1 Oct. - 31 Dec. 1962.

2. Hill, F. K., "Rocket Tunnel Gas Properties," APL/JHU CF 2680, dated Sept. 12, 1957.

3. Steinberg, M. and Davies, W. D., Jour. Chem. Phys. 34, 4, p. 1373, April 1961.

4. Plass, G. N., Jour. Opt. Soc. 49, 8, p. 821, August 1959.

5. Ferriso, C. C., Jour. Chem. Phys. 37, p. 1955, November 1962.

Initial distribution of this document has been made in accordance with a list on file in the Technical Reports Group of The Johns Hopkins University, Applied Physics Laboratory.